



Computational Modelling of the Mechanisms, Kinetics and Thermodynamics of Pyrolysis of Isobutyl Bromide in the Gas-phase

Olubunmi Omolara Adeboye^{1*}

¹Department of Chemistry, Emmanuel Alayande College of Education, P.M.B. 1010, Oyo, Nigeria.

Author's contribution

The sole author designed, analyzed and interpreted and prepared the manuscript.

Article Information

DOI: 10.9734/CSJI/2017/30922

Editor(s):

(1) Yunjin Yao, School of Chemical Engineering, Hefei University of Technology, Tunxi, Hefei, Anhui, China.

Reviewers:

- (1) Nobuaki Tanaka, Shinshu University, Japan.
(2) Vladimir Belyy, Syktyvkar, Komi Republic, Russia.
(3) Vigdergauz Vladimir, INEP KSC Russian Academy of Sciences, Russian Federation.
Complete Peer review History: <http://www.sciencedomain.org/review-history/18540>

Original Research Article

Received 8th December 2016
Accepted 10th February 2017
Published 6th April 2017

ABSTRACT

The kinetics, mechanisms and thermodynamics of the gas-phase pyrolysis of isobutyl bromide at 623 K was carried out using Density Functional Theory modelling with B3LYP at 6-311++G (2df, 2 p) level method of calculation. Calculations showed that the reaction is a unimolecular reaction and the pyrolytic reaction proceeds through a four-centered cyclic transition state that involved a C₁-H₂ and C₃-Br₉ bond breaking and H₂-Br₉ bond making. The calculated data [$\Delta H_{\text{reaction}}$ (48.08 kJ/mol), ΔH^{\ddagger} (205.35 kJ/mol), Ea (210.35 kJ/mol), log A (13.86), rate, k (1.67 x 10⁻⁴ s⁻¹)] obtained at 623 K are in agreement with experimental calculated results at 693 K [$\Delta H_{\text{reaction}}$ (58.61 kJ/mol), ΔH^{\ddagger} (204.83 kJ/mol), Ea (211.01 kJ/mol), log A (13.10), rate, k (1.52 x 10⁻⁴ s⁻¹)] results.

Keywords: Density functional theory calculation; isobutyl bromide; gas-phase; kinetics.

1. INTRODUCTION

Pyrolysis of isobutyl bromide gives 2-methylprop-1-ene and hydrogen bromide. The presence of

C_β - H on the alkyl halide gives gas-phase elimination through a four-centered cyclic transition state mechanism. Gas-phase unimolecular reactions appeared to take place

*Corresponding author: E-mail: moadeb5848@yahoo.com;

through a 4-centered and 6-centered cyclic activated complex [1] but hydrogen halide elimination from the alkyl halides to produce olefins is usually a four-centered reactions. Computational studies on the reactivities of alkyl halides over Al_2O_3 nanoclusters showed that the results are in excellent agreement with the experimental observation, also using the alumina clusters at different sizes with different alkyl halides having β -H for elimination showed that during the elimination pathway the orientation involved a three-centered mechanism with the alumina [2]. Adsorption of series of alkyl halides RX (X=Cl, Br) over acidic zeolite was investigated by ONIOM2 method a 56T model cluster with DFT methods at B3LYP/6-31+G(d,p)genECP:UFF and M062x/6-31+G(d,p)genECP, examining the selective structural changes on the computed adsorption enthalpies of the van der Waals 1:1 adsorption complexes was formed and a modest influence of the halogen atom involved was observed [3]. The mechanisms of the gas-phase elimination kinetics of 1-chloro-3-methylbut-2-ene and 3-chloro-3-methylbut-1-ene and their interconversion was examined by MP2 and DFT levels of calculation, the result obtained was in agreement with experimental parameters showing that elimination reaction occurred in greater rate for 1-chloro-3-methylbut-2-ene and was found to be more thermodynamically stable than 3-chloro-3-methylbut-1-ene [4]. The study of the kinetics and mechanisms [5] of the gas-phase elimination of 2-hydroxyphenethyl chloride and 2-methoxyphenethyl chloride showed that the reaction proceeded through a three-membered cyclic transition state and a four-membered cyclic transition state by the assistance of the aromatic ring. Also, [6] in theoretical study of pyrolytic elimination reaction of ethyl chloride discovered that the results are in agreement with experimental calculated results.

The kinetic, mechanisms, thermodynamics and vibrational calculations carried out on ethyl bromide at 623K [7] using HF at 3-21G, 6-31G* and DFT with B3LYP/6-31G*, 6-311++G (2df, 2p) basis sets showed that the calculated results are in agreement with experimental results. Quantum mechanical calculations of the kinetics, mechanisms and thermodynamics of gas-phase pyrolysis of isopropyl bromide showed that the calculated parameters are also in good agreement with experimental results [8]. In the current study, quantum mechanical calculations were carried out as continuation of the previous study to further explain the influence of bulkiness

of methyl substituent on the rate of pyrolysis of alkyl bromide using isobutyl bromide.

2. COMPUTATIONAL PROCEDURE

2.1 Conformational Search

Molecular mechanics force field (MMFF) was used to carry out conformational search [9,10] to obtain the most stable structure (structure with lowest energy of formation). This is an indication of the stability of the molecule.

2.2 Geometry Optimization

DFT with B3LYP at 6-311++G (2 df, 2 p) level methods of calculation in Spartan 10 were used for the gas-phase elimination reaction. The ground state, transition state and the products were subjected to geometry optimization to obtain the geometric parameters like bond lengths, bond angles, dihedral angles, atomic charges, HOMO/LUMO energy and vibrational properties. These data were used in calculating the kinetic and thermodynamic parameters. The hydrogen that is attached to the β -carbon (H_2) is the hydrogen atom that is to be eliminated. The geometry of the isobutyl bromide is defined in Fig. 1.

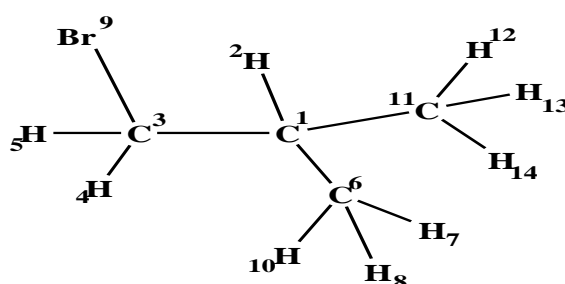


Fig. 1. Geometry of isobutyl bromide

2.3 Reaction Path Studies

$\text{H}_2 - \text{Br}_9$ of the optimized geometry of the isobutyl bromide was set as the reaction coordinate for reaction path calculations. The initial distance (3.044 Å) between $\text{H}_2 - \text{Br}_9$ in its stable reactant form varies to its value (1.440 Å) in the stable product form. This was done by slowly altering the inter atomic distance throughout the calculation of the reaction path in 20 iterations. It was observed that the energy of formation increased to a very high value with a sharp change in the reactant to the product geometry with a sudden drop in the energy of formation to give the approximate value for the

sum of the expected products (hydrogen bromide and 2-methyl prop-1-ene). This is in line with reports on previous work [11].

2.4 Transition State

The saddle point corresponds to the maximum energy, the principle behind this is that there will be interconnectivity by smooth pathways between the reactants and the product through a clearly defined transition state. The guess-transition state in Spartan was used to confirm the suggested mechanism and this was subjected to two tests that could be used to ascertain that a geometry corresponds to a saddle point or a transition state and that this saddle point connects the reactants, the transition state and the products together. The presence of only one imaginary vibrational frequency ($i1052\text{ cm}^{-1}$) within the range of $400 - 2000\text{ cm}^{-1}$ that smoothly connect the reactants and the products together ascertained the transition state. The intrinsic reaction coordinates method was also used, the molecule was optimized subject to a fixed position along the reaction coordinate to perform the two calculations in a positive and negative perturbation along the same normal coordinates.

2.5 Calculations of Kinetic and Thermodynamic Parameters

The statistical mechanically method for calculating enthalpy and entropy to obtain the kinetic and thermodynamic parameters through calculations on the ground state, the transition state and the products are not true representation of the total energy of the molecule hence the sum of the ground state energy (GSE) of molecules and the statistical mechanically calculated energy gives a closer value to the true energy of the molecule. The modified version of the equation to calculate the heat of reaction given below in accordance with [12].

The enthalpy is thus given as:

$$H_i = \text{GSE}_i + H_i^{\text{sm}}$$

Where the 'sm' is the statistical mechanically calculated enthalpy. Putting this equation into the original definition of the heat of reaction we have:

$$\Delta H_{\text{Rxn}} = (\text{GSE}_{\text{product}} + H_{\text{Product}}^{\text{sm}}) - (\text{GSE}_{\text{reactant}} + H_{\text{reactants}}^{\text{sm}})$$

Activation energy (E_a) was calculated according to the transition state theory for a unimolecular reaction at 623K. and it is given as:

$$E_a = \Delta H + RT$$

Entropy of the reaction was calculated by taking the difference of product and reactant entropies.

$$\Delta S_{\text{reaction}} = S_{\text{Product}} - S_{\text{reactants}}$$

Gibbs free energy of activation was calculated using:

$$G = H - TS \text{ and } \Delta G^* = \Delta H^* - T\Delta S.$$

The first order rate constant $k(T)$ was calculated using transition state theory (TST) according to [1] assuming that the transmission coefficient is 1. This is shown in the equation below.

$$k(T) = \frac{k_B T}{h} \exp \left[\frac{-E_a}{RT} \right]$$

Where k_B and h are the Boltzmann and Planck's constants respectively

3. RESULTS AND DISCUSSION

3.1 Geometric Optimization

Geometric optimization (Fig. 2) was performed on the stable structure of isobutyl bromide to obtain the bond lengths, bond angles, dihedral angles (Table 1) and atomic charges (Table 4). The transition state obtained give only one imaginary IR value at vibrational frequency $i1052\text{ cm}^{-1}$ with the intensity at 246.43 and the intrinsic reaction coordinate calculation also shows that the transition state obtained is a true transition state. The bond length between $C_1 - C_3$ in the ground state (GS) (1.526 \AA) shows the length of a carbon-carbon single bond, in the transition state (TS) (1.404 \AA) there is a decrease in the value tending to assume a value for the carbon-carbon double bond in the product (PRD) (1.339 \AA) form. Also, the bond between $C_1 - H_2$ in the GS is 1.095 \AA ; in the TS there is an increase in the value (1.241 \AA) indicating that there is a stretching in the bond length, and in the product, the $C_1 - H_2$ bond does not exist any longer showing that a cleavage has occurred. The $C_3 - Br_9$ bond length in the gs is 1.986 \AA , in the transition state, it has stretched to 2.779 \AA and in the product the bond does not exist any longer showing that a cleavage has also occurred. The bond lengthening between $C_3 - Br_9$ in the TS is higher compared to other bond lengthening; this shows that the cleavage of the bond between $C_3 - Br_9$ is the rate determining step. In the ground state it is observed that there is no bond between

H₂-Br₉ but the bond distance is 3.044Å, the transition state shows that a new bond is forming gradually with bond length (2.122 Å) and the product shows the emergence of a new bond H₂-Br₉ with bond length (1.448 Å). The variation in the bond angles (Table 2) and dihedral angles (Table 3) in the GS, TS and products occurs as a result of the distortion that occur during transformation from reactants to the transition state and finally to the products.

3.2 Atomic Charges

Atomic charges (Fig. 3) in Mulliken are preferred because it gives simple and reasonable estimates of atomic charges [9]. The charges in the TS (Table 4) show that Br₉ has the least charge development while C₁ has the largest (+0.465). The bond polarization between C₁-C₃

facilitates the flow of electron from C₃-Br₉ to enhance the formation of new bond between H₂-Br₉ and the bond polarization of the H₂-Br₉ increase the charge on C₁ atom in the transition state.

Table 1. Bond lengths (Å)

Bond	Ground state	Transition state	Product
C ₁ -H ₂	1.095	1.241	-
C ₁ -C ₃	1.526	1.404	1.339
C ₁ -C ₆	1.539	1.518	1.506
C ₁ -C ₁₁	1.532	1.518	1.506
C ₃ -Br ₉	1.986	2.779	-
C ₃ -H ₄	1.089	1.082	1.085
C ₃ -H ₅	1.088	1.082	1.085
Br ₉ -H ₂	3.044	2.122	1.448

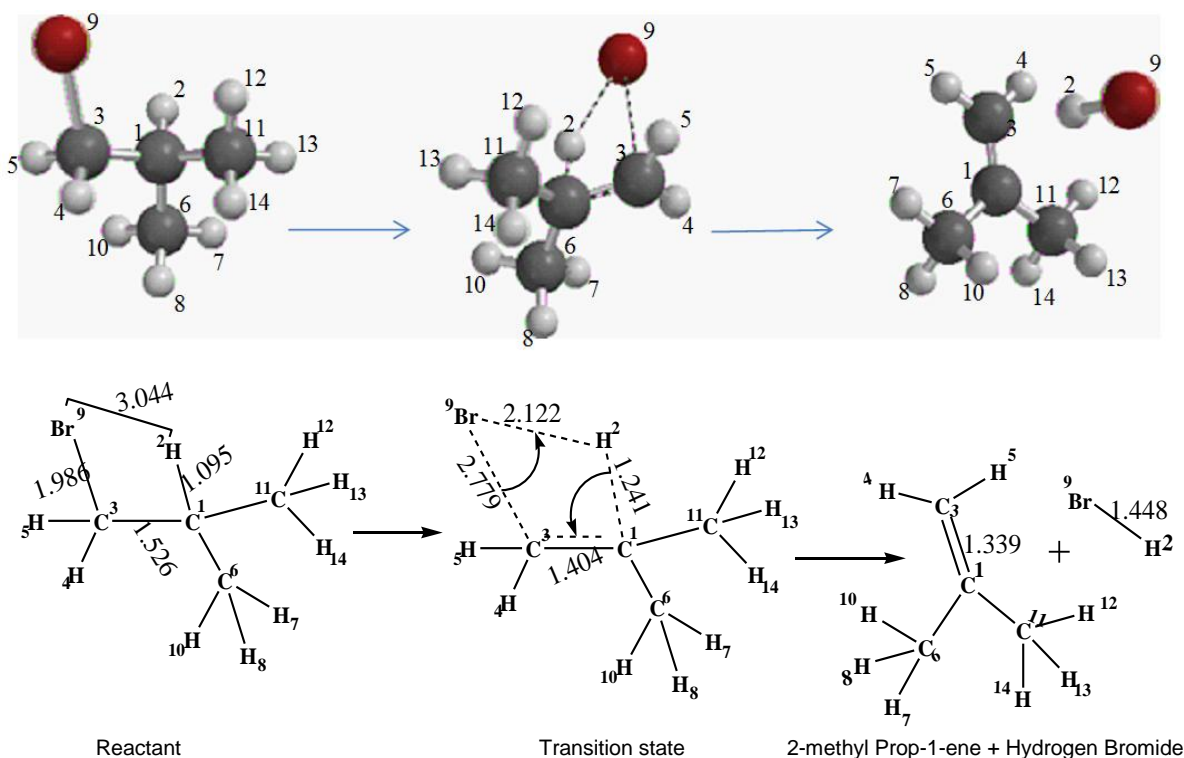


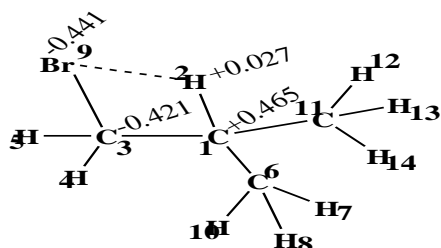
Fig. 2. Optimized geometry of the reactant, transition state and product

Table 2. Bond angles (Å) and energy of formation (kJ/mol)

Bond angles	Ground state	Transition state	Products
C ₃ -C ₁ -H ₂	107.71	72.75	-
Br ₉ -C ₃ -C ₁	113.55	98.20	-
C ₃ -C ₁ -C ₆	112.79	119.76	122.14
C ₃ -C ₁ -C ₁₁	108.28	119.66	122.04
Energy of formation (kJ/mol)	-7171629.67	-7171421.51	-7171580.06

Table 3. Dihedral angles (Å)

Angles	Ground state	Transition state
Br ₉ -C ₃ -C ₁ -C ₆	-171.61	-99.66
Br ₉ -C ₃ -C ₁ -H ₂	-54.97	0.57
Br ₉ -C ₃ -C ₁ -C ₁₁	64.94	101.07

**Fig. 3. Distribution of atomic charges**

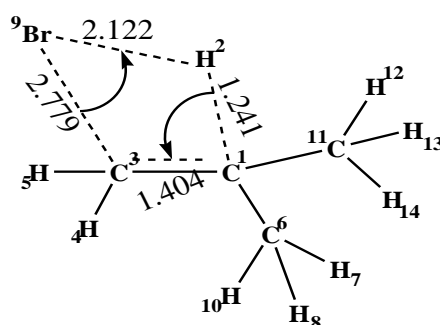
3.3 Mechanism of Pyrolysis of Isobutyl Bromide

The gas-phase elimination reaction of isobutyl bromide proceeds through a four centered mechanism (Fig. 4) which involves a C₃ – Br₉, C₁-H₂ bond breaking and a H₂-Br₉ bond making suggesting C₃ – Br₉ bond (2.779Å) as the rate determining step. The C₁-H₂ in the transition state is stretched (1.241 Å), becomes very long and about to break while the H₂-Br₉ (2.122 Å) is almost fully formed with the bond length between C₃ – C₁ almost assuming a C=C double bond length (1.404 Å) value.

3.4 HOMO and LUMO Energy

Two atomic orbitals interact to give rise to two new molecular orbitals with one of the new orbitals having higher energy than the original (anti-bonding orbital) and the lower one (bonding orbital) in the process of accepting electron when the initial orbital is filled with a pair of electrons and the other is empty, the two electrons can thus be placed in the lower level of the new orbital [13] and this Filled-Empty interaction gives a stabilizing effect. The HOMO, LUMO energy gives insight to the movement of electron in the process of bond breaking and bond formation as revealed in the variation of the HOMO-LUMO gaps in the reactant, transition state and in the products (Table 5): E-HOMO GS [-7.5], TS (-6.3), PRD (-7.3), and E-LUMO GS (-0.6), TS (-3.1), PRD (-0.6)] eV with HOMO-LUMO gap GS [-6.9], TS (-3.2) and PRD (-6.7)] eV. In the HOMO and LUMO surface diagram (Fig. 5). Using frontier molecular orbital theory, electrons are donated from the HOMO of the

nucleophile to the LUMO of an electrophile. The presence of bromine causes a dipole which results in electron density being distributed towards bromine and away from carbon. This thus made the carbon more electrophilic and as a result of the relative placement of the LUMO orbital, the mixing of p-orbital on bromine which is more lower in energy (more electronegative) make it to have poor energy match which is an indication that the energy does not mix as much and therefore makes the LUMO very low and causes the halide ion to leave [14].

**Fig. 4. Structure showing the mechanism of the pyrolysis of isobutyl bromide**

3.5 Kinetic and Thermodynamic Calculations

Kinetic and thermodynamic calculations at 623 K shown in Table 6 for B3LYP/6-311++G (2df, 2 p) ΔH^\ddagger (205.35 kJ/mol), E_a (210.35 kJ/mol), $\log A$ (13.8) and k ($1.67 \times 10^{-4} \text{ s}^{-1}$) are in good agreement with experimental at 693 K [15] results ΔH^\ddagger (204.83 kJ/mol), E_a (211.01 kJ/mol), $\log A$ (13.1) and k ($1.52 \times 10^{-4} \text{ s}^{-1}$). The positive values (48.08 kJ/mol) obtained for the enthalpy of reaction ($\Delta H_{\text{reaction}}$) is an indication that the reaction is endothermic. Also the values obtained for the energy of formation shows that the value obtained for the TS (-7171421.5125 kJ/mol) is closest to the product (-7171580.0625 kJ/mol) than it is to the reactant (-7171629.675 kJ/mol) obeying Hammond postulates to confirm the endothermicity of the reaction. Positive entropy of activation (14.05 J/mol.K) suggests that the activation complex have significant amount of bond cleavages to form two molecules [14]. These values also follow the same trend with isopropyl bromide [8]. The vibrational frequency values obtained (Table 7) and the spectra (Fig. 6) agree with experimental value www.chem.ucla.edu/~webspectra/irtable.html and <http://biochempress.com> [16].

Table 4. Atomic charges

ATOMS	GS	TS	PRD	$\Delta q = TS - GS$
C ₁	+0.213	+0.465	+0.329	+0.252
H ₂	+0.155	+0.027	-0.169	-0.128
C ₃	-0.330	-0.421	-0.446	-0.091
H ₄	+0.166	+0.216	+0.138	+0.050
H ₅	+0.174	+0.217	+0.136	+0.043
C ₆	-0.512	-0.502	-0.527	+0.01
H ₇	+0.144	+0.154	+0.141	+0.01
H ₈	+0.136	+0.152	+0.145	+0.016
Br ₉	-0.145	-0.441	-0.150	-0.296
H ₁₀	+0.146	+0.165	+0.156	+0.019
C ₁₁	-0.556	-0.504	-0.530	+0.052
H ₁₂	+0.136	+0.154	+0.140	+0.018
H ₁₃	+0.139	+0.151	+0.153	+0.012
H ₁₄	+0.133	+0.166	+0.145	+0.033

Table 5. HOMO/LUMO energy

States	HOMO	LUMO	(HOMO-LUMO Gap)
Reactant	-7.5	-0.6	-6.9
Transition state	-6.3	-3.1	-3.2
Product	-7.3	-0.6	-6.7

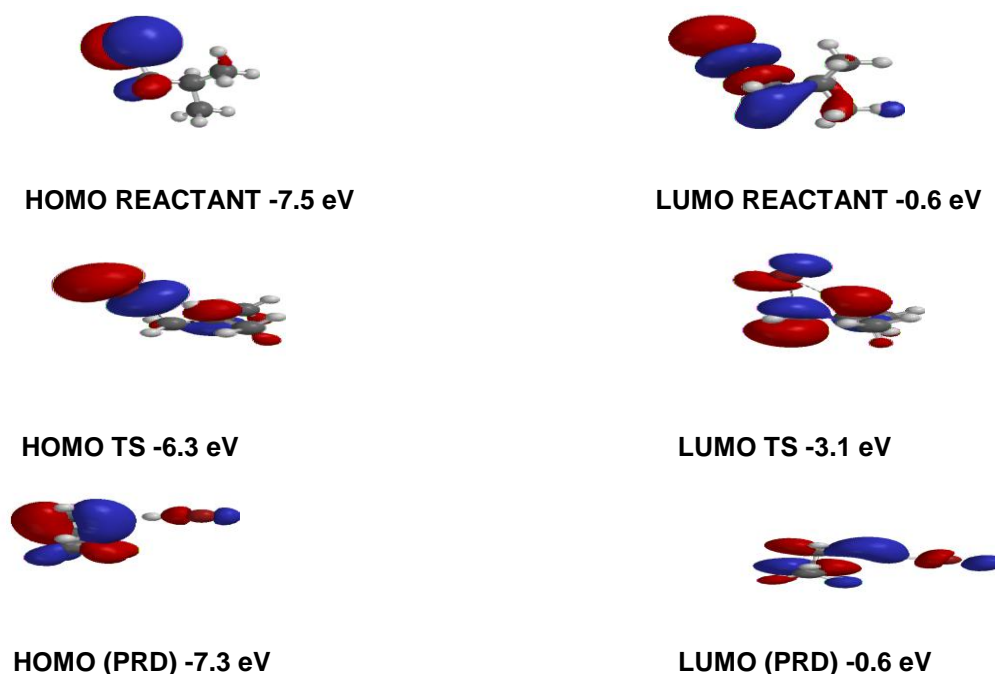


Fig. 5. HOMO/LUMO density surface diagram for the reactant, transition state and products for isobutyl bromide

Comparing the data obtained for calculated rate constant, $k = 6.6 \times 10^{-3}$ for isopropyl bromide [8] and for isobutyl bromide ($k = 1.67 \times 10^{-4}$) there is an indication that rate of pyrolysis is higher in

isobutyl bromide because of the cumulative inductive effect caused by the methyl groups. The trends of the results obtained is in line with experimental calculated results.

Table 6. Kinetic and thermodynamic parameters at 623k

Parameters	Experimental values	Calculated values
$\Delta H_{\text{reaction}}$ (kJ/mol)	58.61	48.08
$\Delta S_{\text{reaction}}$ (J/mol.K)	N/A	22.03
ΔS^{\ddagger} (J/mol.K)	N/A	14.05
ΔH^{\ddagger} (kJ/mol)	204.83	205.35
ΔG^{\ddagger} (kJ/mol)	N/A	196.62
Ea (kJ/mol)	211.01	210.35
log A	13.10	13.86
Rate k (s ⁻¹)	1.52 X 10 ⁻⁴	1.67 X 10 ⁻⁴

Experimental values Ref: Harden and Maccoll, 1959

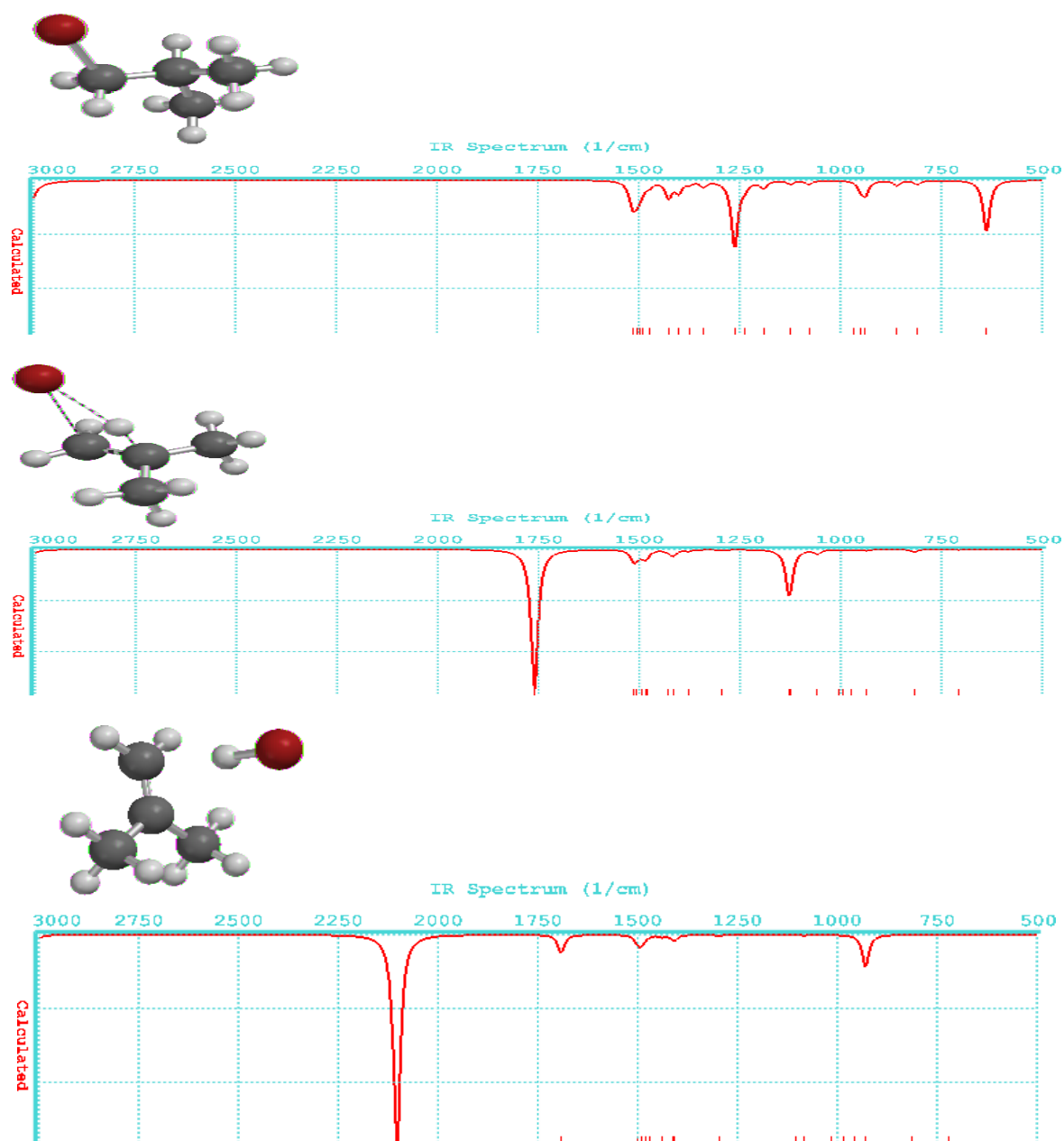


Fig. 6. Spectra of the reactant, transition state and product respectively

Table 7. Vibrational frequency (cm⁻¹)

	Experimental values	Calculated values
REACTANT		
$\nu(\text{C-H})_{\text{bending}}$	985-1000	1031-1410
$\nu(\text{C-H})_{\text{stretching}}$	3101-3010	2978 -3167
PRODUCT1(2-Methylprop-1-ene)		
$\nu(\text{C-H})_{\text{bending}}$	988-1010	1004 -1442
$\nu(\text{C=C})_{\text{stretching}}$	1620-1700	1869
$\nu(\text{C-H})_{\text{stretching}}$	3010-3100	3022 -3158
PRODUCT2 (Hydrogen Bromide)		
$\nu(\text{H-Br})$	2348	2439

4. CONCLUSION

Computational modelling could be used to effectively predict that as the bulkiness and branching of methyl substituent increases the rate of pyrolysis of alkyl halide to form alkenes also increases. This is shown in the result comparing the previous calculated result on isopropyl bromide with the calculated result on isobutyl bromide.

COMPETING INTERESTS

Author has declared that no competing interests exist.

REFERENCES

- O'Neal HE, Benson SW. A method for estimating the Arrhenius, A factor for four and six – center unimolecular reactions. *Journal of Physical Chemistry*. 1967;71(9): 2911.
- Biswas S, Pramanik A, Sarkar P. Computational studies on the reactivity of alkyl halides over (Al₂O₃)_n nanoclusters: An approach towards room temperature dehydrohalogenation. *E Pub Nanoscale*. 2016;8(19):10205-18.
- Agnies MK. Adsorption enthalpy of alkyl halides in a FAU acidic zeolite investigated by the ONIOM2 method. *Journal of Theoretical and Computational Chemistry*. 2015;14(5). DOI:<http://dx.doi.org/10.1142/S0219633615500340>
- JesUs Jose L, Edgar R, Tania Cordova M, Gabriel Chuchani. DFT and ab-initio study on the mechanism of the gas-phase elimination kinetics of 1-chloro-3-methylbut-2-ene and 3-chloro-3-methylbut-1-ene and their isomerization. *Journal of Computational Methods in Sciences and Engineering* 12; 2012. DOI: 10.3233/JCM-2012-0412.
- Brusco Y, Berroteran N, Loroño M, Córdoba T, Chuchani G. Theoretical calculations for neighboring group participation in gas-phase elimination kinetics of 2-hydroxyphenethyl chloride and 2-methoxyphenethyl chloride. *J. Phys. Org. Chem*. 2009;22:1022–1029.
- Adejoro IA, Emmanuel Ekeh. Theoretical study of the kinetics of the pyrolytic elimination reaction of ethyl chloride. *E- Journal of Chemistry* 2010;7(1):271–274.
- Adejoro IA, Adeboye OO, Esan T. Ab-initio and DFT studies of the kinetics, mechanisms and thermodynamics of the gas-phase pyrolysis of ethyl bromide. *African Journal of Pure and Applied Chemistry*. 2013;7(6):231-241.
- Adeboye OO. Quantum mechanical study of kinetics, mechanisms and thermodynamics of the gas-phase pyrolysis of Isopropyl Bromide. *IISTE: Chemistry and Material Research*. 2014;6 (10):1-9.
- Warren Hehre J. A guide to molecular mechanics and quantum chemical calculations. Irvine USA. 2003;399.
- Warren hehre and sean ohlinger. Spartan '10 Tutorial and user's guide. Wavefunction Inc; 2010. ISBN 978-1-890661-41-4
- Mclver JW, Jr. Kormonicki A. Rapid geometry optimization for semi- empirical molecular orbital methods. *Chem. Phys. Letts*. 1971;10:303.
- Spartan Calculation Guide. Available:www.engin.umich.edu/~cre/web_mod/quantum/topic03.htm
- Madhhavan J. Arulmozhi S, Victor anthony Raj HOMO, LUMO analysis and first order hyperpolarizability of 2-amino-5-chlorobenzophenone using computational methods.

- Pelagia Research Library Der Chemica. 2011;2(6):158-163.
14. Anslyn EV, Dougherty DA. Modern organic chemistry. University Science Books USA; 2006.
Available:www.uscibooks.com 368
 15. Harden GD, Maccoll A. Studies in the pyrolysis of organic bromides. Part XIII. The limiting rate of decomposition of isobutyl bromide in the presence of inhibitors. J. Chem. Soc. 1959;97-1200.
DOI: 10.1039/JR9590001197
 16. Martin Grayson. The infrared and raman spectroscopic signals of HF, HCl, HBr and HI. International Electronic Journal of Molecular Design. BioChem Press. 2003;2.
Available:<http://biochempress.com>

© 2017 Adeboye; This is an Open Access article distributed under the terms of the Creative Commons Attribution License (<http://creativecommons.org/licenses/by/4.0>), which permits unrestricted use, distribution, and reproduction in any medium, provided the original work is properly cited.

Peer-review history:
The peer review history for this paper can be accessed here:
<http://sciencedomain.org/review-history/18540>